2021

Integrated Thermal Energy Storage System For Air-conditioners With Phase-Change Composites

Anurag Goyal
National Renewable Energy Laboratory, United States of America, Anurag.Goyal@nrel.gov

Eric Kozubal

Jason Woods

Integrated Thermal Energy Storage System for Air-conditioners with Phase-change Composites

Anurag GOYAL*, Eric KOZUBAL, Jason WOODS

Building Energy Science Group
National Renewable Energy Laboratory, Golden, CO, USA
Contact Information - Email: Anurag.Goyal@nrel.gov, Ph: 303-384-6451
* Corresponding Author

ABSTRACT

Thermal energy storage (TES) is a promising solution to store and dispatch energy and shave peak electric load, reducing the operational cost of HVAC systems. We present results of a TES system using phase-change materials (PCM) integrated with an air conditioner. The proposed system uses an organic PCM (tetradecane) encapsulated within compressed expanded natural graphite foams referred to as phase-change composite. The graphite foam encapsulates the PCM eliminating the need for expensive storage vessels, reduces installation costs, and provides higher thermal conductivity that can lead to faster charge/discharge rates. Two serpentines, multi-pass circuits, operating as a heat source and a sink, exchange heat to and from the phase-change composite. These two circuits are embedded in multiple slabs of this material. The "charge" circuit contains the refrigerant that is directly coupled to a vapor compression system, and the "discharge" circuit removes heat from an airstream and releases it into the PCM composite through a water-glycol liquid coupling. This configuration allows for multiple modes of operation depending on the state of charge of the thermal energy storage module, the building air-conditioning load, and the current electricity and demand charges. This flexible operation allows variable air volume capacity control without the need to have a variable capacity refrigeration system. We developed a 21 kW-hr (6 RT-hr) prototype TES system coupled with a commercial air-conditioner to characterize the component- and system-level performance.

1. INTRODUCTION

The rapid penetration of on-site renewable generation for buildings has led to new requirements for sustaining the integrity of the electric grid. Flexible resources are needed for this paradigm, which could include behind-the-meter energy storage assets at buildings. These assets enable utility customers to respond to price signals, whether peak-demand charges, time-of-use electricity rates, real-time pricing, or demand response signals [1]. This new paradigm requires increased flexibility in how these storage assets are used. Thermal energy storage (TES) in heating, ventilation, and air-conditioning (HVAC) systems can help mitigate energy and demand costs for building owners by lowering energy demand during high-price periods.

Traditional TES systems for building cooling, e.g., Calmac [2], use ice as the PCM to store energy and provide cooling. Due to the lower freezing point of ice than typical air-conditioning temperatures, the chiller system operates at a reduced efficiency which negatively impacts the round-trip efficiency of the integrated system. These systems are typically designed and built for large capacity installations with central chiller plants. Due to their higher weight and capital cost, these systems are not feasible for smaller rooftop units (RTUs), but these RTUs condition a larger fraction of commercial floor space than the central chiller plans. Moreover, conventional TES systems typically involve a single fluid circuit (water-glycol coolant) which is either used to provide direct cooling from the chiller to the building or is used at night time to freeze ice and store energy for use during the day. These systems reduce day-time energy use by charging at night, but what is needed is a more flexible technology that can shave/shift on-peak air conditioning load, improve efficiency, and dynamically charge or discharge in response to expected grid operating levels and time scales [3-6].

This paper presents a technology that could meet these needs—a hybrid TES integrated RTU air conditioner as shown in Figure 1(a). The system consists of two fluid circuits: a refrigeration circuit that charges (freezes) a phase-change composite of n-tetradecane with compressed expanded natural graphite (CENG) foam using the evaporating refrigerant. A second circuit in the PCM is used to discharge (melt) the material and rejects heat from a cooling coil using a glycol circuit [7]. This dual-circuit design allows greater flexibility in utilizing the thermal storage system during dynamic grid operating conditions. Moreover, the shape-stable composite of graphite and n-tetradecane offers several advantages over conventional PCMs such as ice. First, the freezing point of this material is ~4.5°C which improves the overall efficiency of the HVAC system. Second, the composite of graphite foam and the PCM provides

high thermal conductivity to improve the charge/discharge rates. And, third, the shape stable composite helps encapsulate the PCM in its pores and eliminates the need for expensive tanks to store the material. We present the measured and modeled performance of the current state of this technology, and its potential future performance as integrated with an RTU. The proposed solution minimizes the weight of the integrated system by using a smaller capacity TES system compared to traditional ice-based systems for peak load shifting, ~(14-25 kWh) for a 17.5 kW (5 RT) RTU, to flatten the load during peak hours (Figure 1(b)). The system can be integrated into the RTU at the factory, reducing integration costs and maintaining a similar installation procedure to standard systems, and reducing the reluctance of RTU installers and building owners to adopt new technologies. We identify the limitations in the performance of the developed prototype, improvements for future system designs, and evaluate scenarios for flexible load shaving and operation.

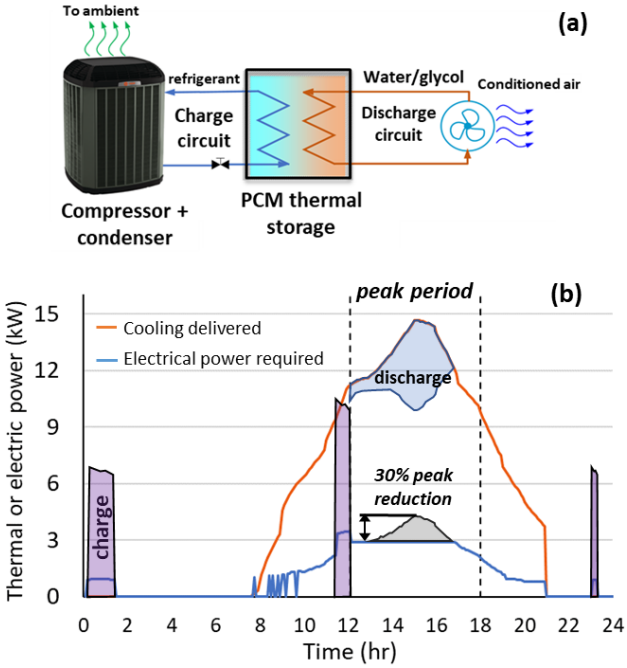

Figure 1*:* (a) Dual-circuit c-PCM HX integrated with air conditioner, (b) modeling results showing 30% peak reduction by adding a 14 kWh storage to a 17.5 kW variable-speed rooftop unit.

2. THERMAL ENERGY STORAGE SYSTEM

The proposed system consists of a primary refrigeration circuit with a secondary loop heat exchanger that has embedded composite phase- change composite as shown in Figure 1. The composite PCM uses a high porosity compressed expanded natural graphite (CENG) foam to contain the PCM used in the prototype system (n-tetradecane). The CENG foam produces a shape-stable composite that has solid-like properties (i.e. it does not flow). The foam also enhances thermal conductivity by about 100 times that of the pure PCM [8].

Figure 2 shows a 3-D CAD drawing and photograph of one module. The module consists of 12 slabs of composite PCM with alternating discharge (22% Ethylene Glycol) and charge (R410a) fluid circuits. The dimensions of an individual slab are 0.520 m × 0.460 m × 0.035 m (L×W×H). Copper tubes of 0.0095 m (3/8 in) outer diameter were

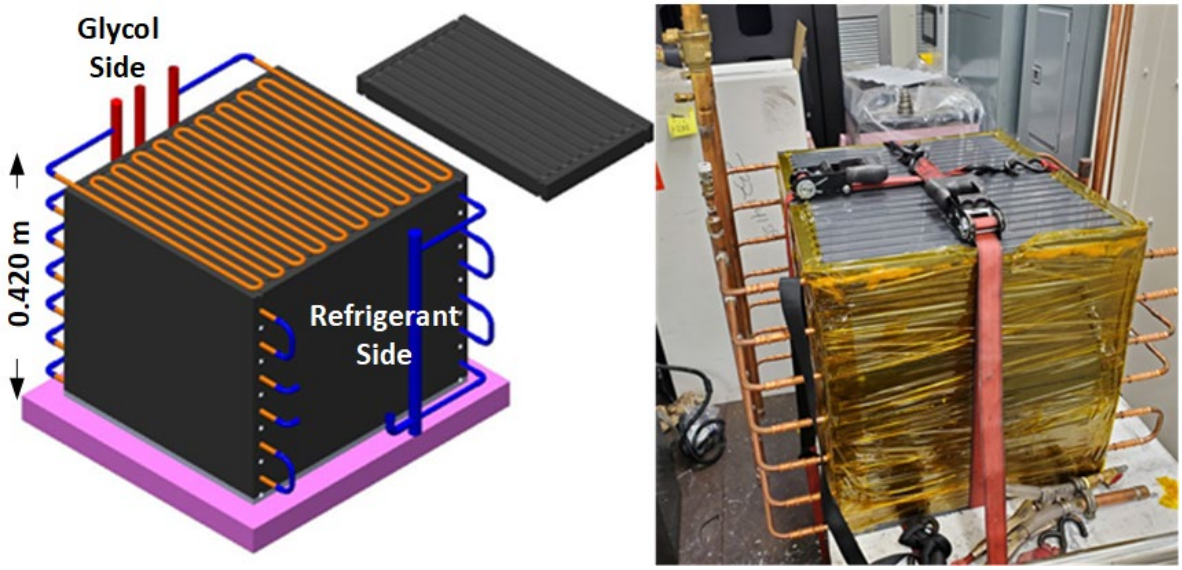

Figure 2*: 3-D CAD rendering (left) and the fabricated thermal energy storage module (right)*

used for both fluid circuits. The fluid circuits formed a 20-pass serpentine path in each row. A total of 13 tubes (7 discharge, 6 charge) were used. There were 7 single-pass discharge circuits and 2 three-pass charge circuits. The design of the thermal energy storage (TES) modules rely on the thermal conduction path between the two fluid circuits. Thus, the thermal conduction of the graphite foam along with the contact conductance between the copper tubes and the composite material are critical factors in the performance of this design. For the system to operate efficiently, these conductance values should be maximized.

3. METHODS

3.1. Experiments

A commercial RTU of 21.1 kW_{th} nominal cooling capacity was modified to fabricate the prototype hybrid unit. There are three sub-systems: a charging subsystem, a discharging subsystem, and the TES subsystem (Figure 3).

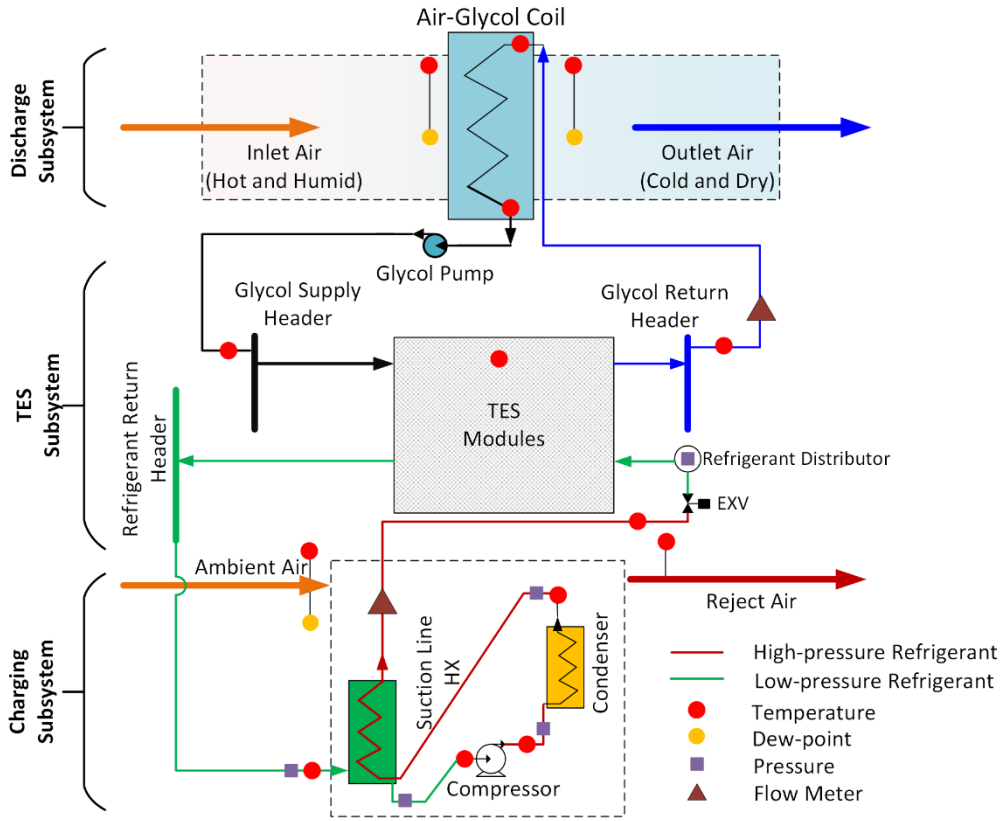

Figure 3*: Schematic of the prototype 5RT system with instrumentation*

The **charging subsystem** delivers high-pressure liquid refrigerant to the TES and receives low-pressure vapor from the TES. The subsystem consists of a re-purposed split system condensing unit which was modified with a variable speed compressor, suction-line heat exchanger, and a refrigerant accumulator. The suction-line heat exchanger and the integrated accumulator provided refrigerant superheating and prevented liquid-phase refrigerant from entering the compressor. The instrumentation allowed measurement of refrigerant temperatures, pressures, and mass flow rate. The charging subsystem allows for variable control of charging to one of the following modes:

1. Constant charging capacity – maintain a constant heat removal rate from the TES
2. Constant charging temperature – maintain a constant evaporator saturated temperature
3. Constant volumetric capacity – simulate a single- or multi-speed compressor

Figure 4 shows five identical TES modules connected to the refrigeration system (charging circuit) and the air-handling system coupled through a water-glycol loop (discharge circuit). The refrigeration system is connected to the TES modules such that the total refrigerant and glycol flow are equally divided and supplied to these modules at identical inlet conditions. We instrumented these modules to measure temperatures at various locations. All

measurement probes and actuators were connected to the data acquisition and control system in the laboratory to collect experimental data and implement control algorithms.

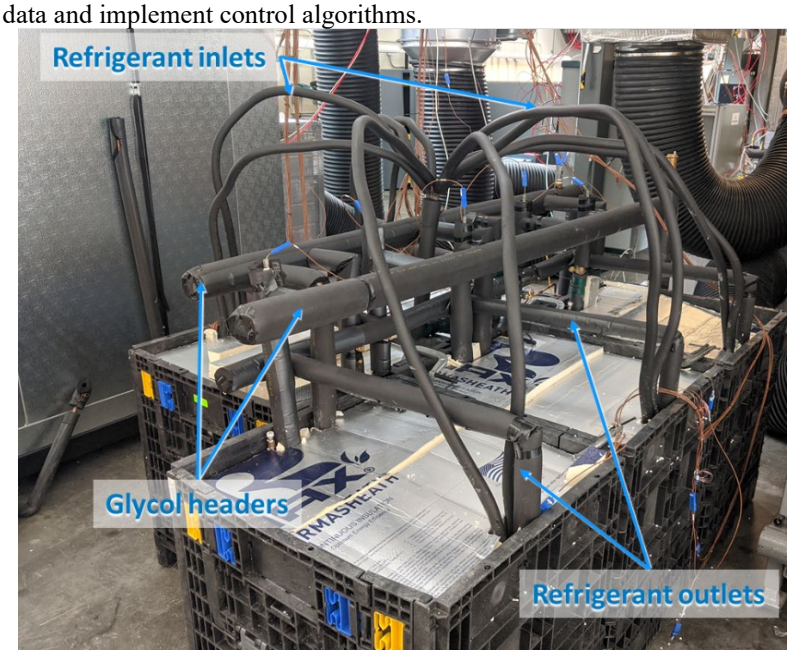

Figure 4: *Thermal energy storage modules connected to the air-conditioning and air-handling system*

The **discharge sub-system** cools a building space using a standard chilled water-glycol coil. Since refrigeration temperatures were expected to be as low as -8°C during experiments, 22% ethylene glycol was used. This subsystem consists of the water-glycol coil, a variable speed glycol pump, and a pair of variable speed fans packaged in an air handling unit. The design intent was to receive 8°C chilled glycol from the TES to cool 2000 CFM of process air to provide 17.6 kW_{th} of cooling. Because the TES system delivers near-constant temperature glycol, the cooling capacity is modulated by changing the air and glycol flow rates. Reducing air and glycol flow during lower-load conditions thus translates to air temperature and humidity dropping below that of the design condition. This provides the benefit of delivering air at a dewpoint less than about 13°C at all operating points and maintaining an acceptably low sensible heat ratio (ratio of sensible heat removal to total heat removal). This combination of modulation capacity (down to about 20% of full load capacity) and constant supply air dewpoint creates a system with good humidity control. In hot/dry climates, where humidity control is not a primary concern, the air flow rate can be increased to maintain total capacity and deliver a higher sensible heat ratio.

The laboratory provides air at the desired temperature and humidity to simulate different indoor and outdoor conditions. Airstreams were connected to the charge- and discharge-side of the system with measurements of dry bulb and dew point temperature, and volumetric flow rates. Pressure and temperature probes at several locations of the refrigerant circuit allowed us to fully define the thermodynamic state of the working fluid. With the measured mass flow rate of the refrigerant, the heat transfer rate in an individual component is estimated as:

$$\dot{Q}_{ref} = \dot{m}_{ref}(h_{ref,out} - h_{ref,in}) \tag{1}$$

We also measured the temperature and the volumetric flow rate of the glycol-water mixture in the discharge circuit. Heat transfer rate on the discharge side is calculated using:

$$\dot{Q}_{glycol-water} = \dot{m}_{glycol-water} Cp_{glycol-water}(T_{glycol-water,in} - T_{glycol-water,out}) \tag{2}$$

We also instrumented the thermal energy storage modules with 31 embedded thermocouples to estimate the state of charge (SOC) of the system. We installed 24 surface-mounted thermocouples on tubes supplying fluids to the modules which helped quantify circuit-to-circuit fluid distribution.

Due to the large thermal inertia of thermal energy storage, a custom control algorithm was designed to operate the electronic expansion valve on the refrigerant circuit. The algorithm uses a combination of a feedforward controller based on a predictive model of the flow through the valve and a feedback controller as a corrector to achieve the setpoint of refrigerant superheat at the inlet of the compressor.

The **TES subsystem** functions as a thermal buffer between the charge and discharge sub-systems. The modules allow the system to follow building thermal loads and maintain the thermal comfort of the occupants while managing energy

and power draw from the electric grid. The modules contained 24.2 kWh of thermal storage capacity calculated from an isothermal temperature from -2°C to 15°C. The two-fluid circuits thermally connect the phase change material, the glycol stream, and the refrigerant stream (evaporator). In the prototype design, the TES heat exchanger was dictated by existing manufacturing constraints and consisted of the serpentine design discussed above. The repeating stacking of the tubes and composite PCM was as follows: glycol serpentine – 35mm PCM slab – refrigerant serpentine – 35 mm PCM slab. The thermal network dictates that the heat flows from the glycol, through the composite PCM, and into the refrigerant.

The prototype system design allowed for measured thermal performance of each of the sub-systems, and to discover the potential for design improvement. Given this, the system design was intended to provide the following functionality:

1. 17.6 kW_{th} net cooling capacity at ASHRAE standard conditions
2. > 1.2 hours of thermal energy storage
3. During full load hybrid mode, the TES should provide at least 1/3 of the peak cooling capacity throughout its discharge. This equates to delivering 10°C chilled water at a discharge rate of ~ 6 kW_{th}.
4. Efficient TES module charging is critical to overall energy use and utility costs. The TES was designed to maintain less than a 5°C approach between refrigerant evaporator temperature and the TES module temperature at 17.6 kW_{th} charge capacity.

The refrigeration cycle efficiency is sensitive to the saturated evaporator temperature. Using a simplified Carnot analysis on a refrigeration cycle (assuming an ambient heat sink temperature of 35°C, two evaporator temperatures of 10°C and 9°C, and isentropic efficiency of the compressor as 65%), we obtain that every 1°C decrease in evaporator temperature increases energy use by 0.09 kW for a 17.6 kW_{th} cooling system. Thus, a drop by 1°C in average evaporator temperature results in about a 4.1% increase in average energy consumption. This penalty is inherent in an air conditioning system with a secondary fluid coupling. Minimizing its effect is critical toward managing energy and power use. It is not conclusive here that the overall COP of the integrated system with TES will increase, but it will change as the evaporator and condenser temperatures vary. The former is impacted by the additional approach temperature due to the TES heat exchanger, and the second is impacted by ambient temperature. The combined system will benefit from using higher transition temperature phase-change material to maintain a high evaporator temperature and from charging the system at night time when the ambient temperatures are lower.

3.2. Numerical Modeling

We developed a finite-volume numerical model of the heat transfer process within the TES module following the approach presented in [7]. Figure 5 shows the computational domain and geometry of a single control volume (CV). Each CV consists of the composite PCM along the pass of the tube over the total depth of the module, and exchanges heat with the fluid flowing in the copper tubing. As thermal storage is inherently an unsteady phenomenon, the conservation laws in their unsteady form are used.

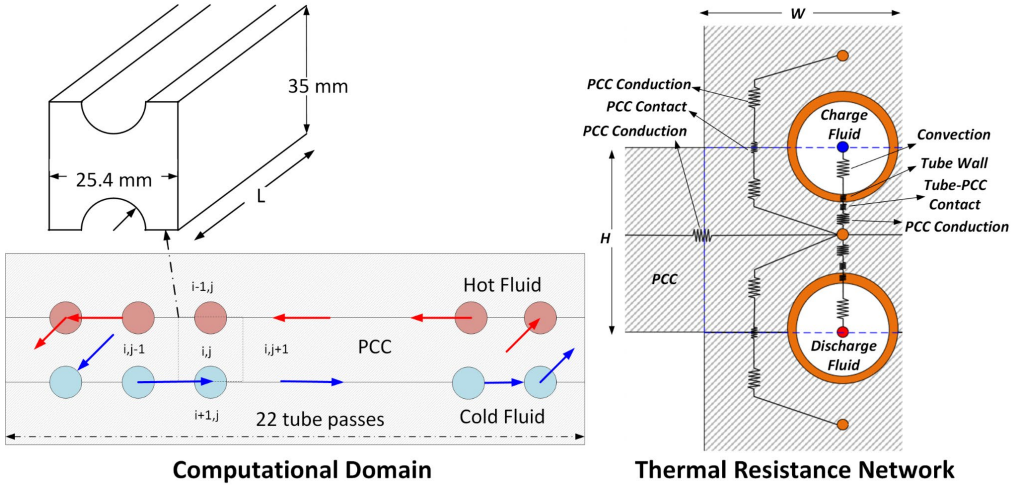

Figure 5: *Computational domain and thermal resistance network* [7]

We assumed the following to simplify the governing equations:

- fluid flow is assumed to be one-dimensional and incompressible

- viscous dissipation and body forces are neglected,
- dynamic variations in pressure are neglected and a static formulation of pressure loss is used over each control volume during every time step,
- effects of axial conduction are neglected in the fluid as the Peclet (Pe) number is typically large,
- constant cross-sectional area of fluid flow,
- uniform heat transfer coefficient assumed in the control volume for both fluids,
- refrigerant flow is assumed to be at a quasi-steady state with saturated vapor at the outlet of the module,
- heat transfer in the composite PCM is modeled as two-dimensional conduction from the adjacent nodes,
- The graphite-tetradecane composite is modeled as a single material with one set of material properties,
- lumped capacitance is used for each PCM volume, (Biot number ~0.2)
- heat transfer from curved tube surface to the PCM is modeled using an empirical shape factor for heat conduction, and
- finite thermal contact resistance is used at the interface between the tube and the PCM volume and between PCM volumes.

These assumptions simplify the conservation laws and the energy conservation equations for the two fluids and the composite PCM, and the static pressure drop equation is used per node to formulate the system of discretized equations. We use a thermal resistance network formulation to resolve different convective and conductive heat transfer media. Figure 5 shows a single control volume with both fluid tubes and the PCM volume. Heat transfer paths from the hot fluid to the cold fluid through various materials and interfaces account for the different thermal resistance terms discussed below.

The model initiates with an initial condition of module and fluid temperatures at thermal equilibrium and uses time-dependent boundary conditions of fluid inlet temperatures and flow rates as inputs. The system of discretized equations is solved at each time step to predict fluid outlet temperatures, nodal fluid and PCM temperatures, and the heat transfer rate through each fluid circuit. Material properties for the thermal energy storage material are listed in Table 1.

Table 1: *Thermophysical properties of tetradecane-graphite composite for TES*

Property	Value
Transition Temperature	~4.5°C
Density	836.1 kg m^{-3}
Porosity	~90%
Enthalpy of Phase-change	~168 kJ kg^{-1}
Thermal Conductivity (in-plane direction)	18 W m^{-1} K^{-1}
Thermal Conductivity (primary heat transfer direction)	10 W m^{-1} K^{-1}

4. RESULTS AND DISCUSSION

4.1. Charging

During charging, the refrigerant circuit was operated to provide cold refrigerant to remove energy from the thermal energy storage modules. The system was charged at a constant refrigerant temperature of -2 °C, and condenser air temperature of 35 °C and a flow rate of ~4500 CFM. As the system SOC increased during charging, the refrigerant temperature and consequently pressure continuously decrease. To prevent reaching the low-pressure limit on the compressor and potentially reaching the freezing point of the water-glycol mixture in the discharge loop, we controlled the refrigerant temperature (pressure) to stay above a lower limit at the compressor inlet. The results from one of these experiments are shown below. Figure 6 shows the heat transfer rate, the total energy stored, and the COP of the system as a function of time. During charging the heat transfer rate decreased (remaining nearly constant at ~7 kW for the bulk of the phase-change process) as the driving temperature difference in the system decreased. The total energy stored was ~25 kW-hr. In this process, the system COP remained at ~2.75. The COP of the system during charging is defined as:

$$COP_{charging} = \frac{\dot{Q}_{ref,TES}}{\dot{W}_{elec,cond,fan} + \dot{W}_{elec,comp}} \tag{3}$$

Figure 7 shows the performance of the system as a function of the SOC. During the initial phase of charging (starting at ~15 °C isothermal conditions in the thermal energy storage modules or a SOC of 0%), the compressor operated at the maximum allowable speed of 5000 RPM before it was modulated to maintain the refrigerant temperature limit. As the system SOC increases, the heat transfer resistance between the refrigerant and the liquid-solid phase-front

increases, leading to a decrease in the heat transfer rate during charging at a constant refrigerant temperature. The compressor speed decreases in response to this to maintain a constant refrigerant temperature. The system was charged to 100% SOC when the majority (>80%) of the embedded thermocouples inside the modules recorded a temperature below -2°C.

The system COP is the ratio of heat transferred into the thermal energy storage modules and the electrical input to the system (compressor and condenser fan power). The system COP during charging was ~2.75 primarily due to the low refrigerant temperature.

In other experiments, the COP of the system was observed to increase at higher refrigerant temperatures, as expected. As per the original concept, the evaporator temperature was anticipated to be only 2-5°C lower than the transition temperature at the measured heat transfer rates. But due to high contact resistance, the refrigerant temperature had to be lowered to achieve the target heat transfer rate which led to lower efficiency of the refrigeration system.

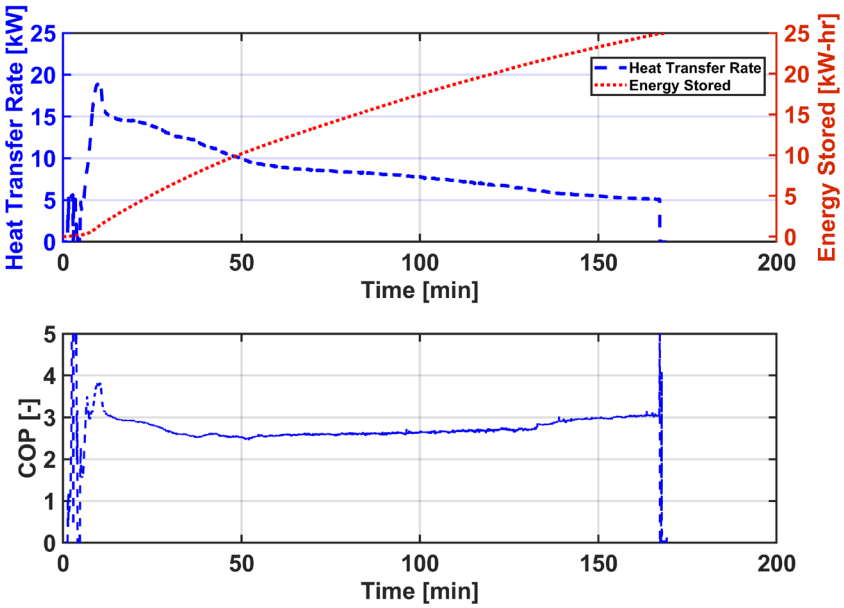

Figure 6: *Heat transfer rates and energy stored in the TES heat exchanger with a saturation temperature of -6* °C

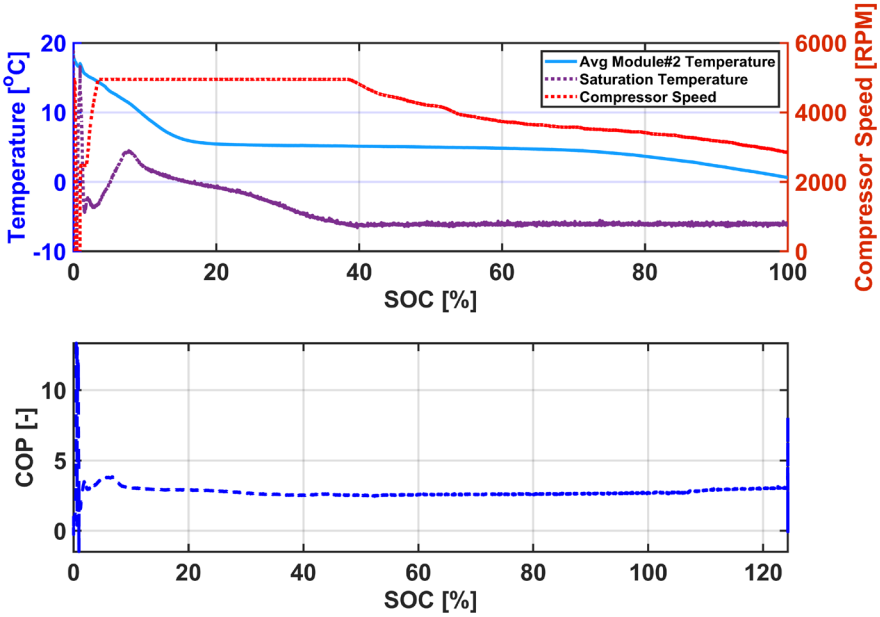

Figure 7*: System performance as a function of SOC during charging at -6°C*

4.2. Discharging

After charging, the system was left overnight to equilibrate the temperature differences present in the PCM after the completion of charging. This allowed for isothermal initial conditions before the discharge experiment the next day. The system was discharged at AHRI 210/240 standard conditions with the inlet air set at 26.7°C dry bulb temperature, 15.8°C dew point temperature, and 2000 CFM flow rate. As the system SOC decreased during discharging, the glycol supply temperature and the air outlet temperature from the modules increased as shown in Figure 8. As the supplied air temperature increases, the performance of the system was analyzed by setting a cutoff temperature of the glycol-water mixture supplied by the modules. This also allows comparing different discharging experiments.

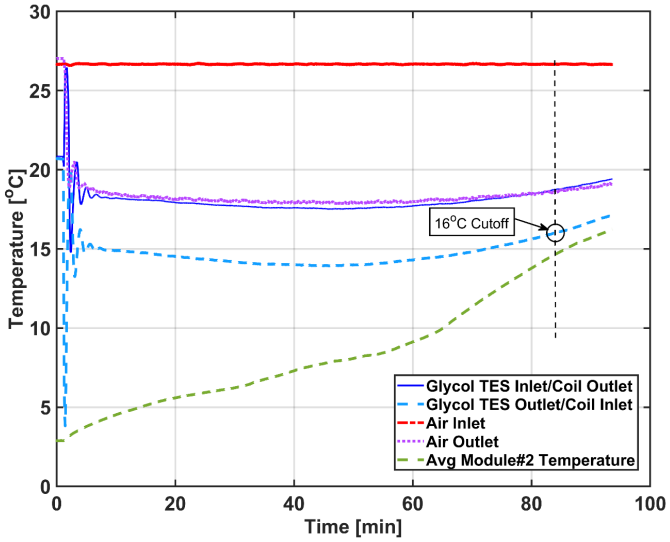

Figure 8*: Air, glycol, and module temperatures during discharge at AHRI standard conditions*

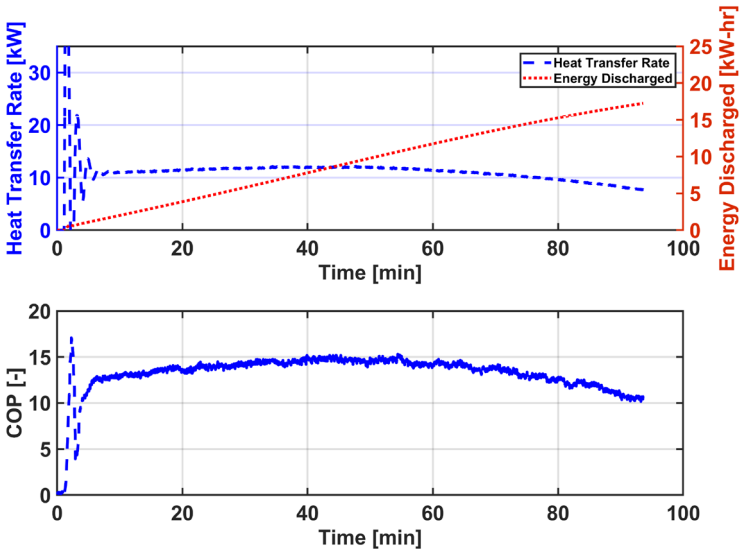

Figure 9: *Heat transfer and energy storage performance of the system during discharge at AHRI standard conditions*

Figure 9 shows the heat transfer and energy discharged from the system. During the majority of the discharging, the system delivered a cooling capacity of ~12.32 kW RT and 15.87 kW-hr of total discharged energy until reaching the cutoff glycol temperature. The system COP during discharging is calculated as the ratio of heat transferred to the glycol stream and the electrical input to the system (glycol pump and fan power). The discharge COP was about 15. During discharging no latent cooling (moisture removal) was observed in the air stream. This is due to the relatively

high inlet glycol temperature entering the cooling coil. This high temperature is a result of higher than anticipated thermal resistance between the glycol circuit and the thermal energy storage material. We used the numerical model, described in Section 3, in conjunction with experimental data to estimate thermal contact resistances within the TES module. Our calculations show that the contact resistances between the copper-tubes and the phase-change composite material, and between different slabs of the material are the most dominant thermal resistances accounting for more than 50% of the total thermal resistance. With improved thermal contact between the fluid tubes and the thermal energy storage, better heat transfer rates and energy utilization can be achieved from the system.

4.3. Hybrid Operation

We operated the prototype system in hybrid mode (simultaneous charging and discharging) to demonstrate the operational flexibility of this design as compared to existing TES systems. Figure 10 shows results from one operating scenario that was simulated where the delivered cooling capacity is held constant while the compressor power can be modulated to achieve partial load shaving. The delivered cooling capacity is held steady at ~10 kW, while the compressor speed changes from 4700 RPM, to 2700 RPM, and then turns off (Figure 10 (a)). During these three phases, the TES system is being charged at 2.46 kW, discharged at 2.29 kW, and then discharged at ~10 kW, respectively (Figure 10 (b)). Figure 10 (c) shows the corresponding variation in the state of charge of the TES module. This hybrid operation enables the partial load shaving shown in Figure 1(b), without needing additional valves or heat exchangers.

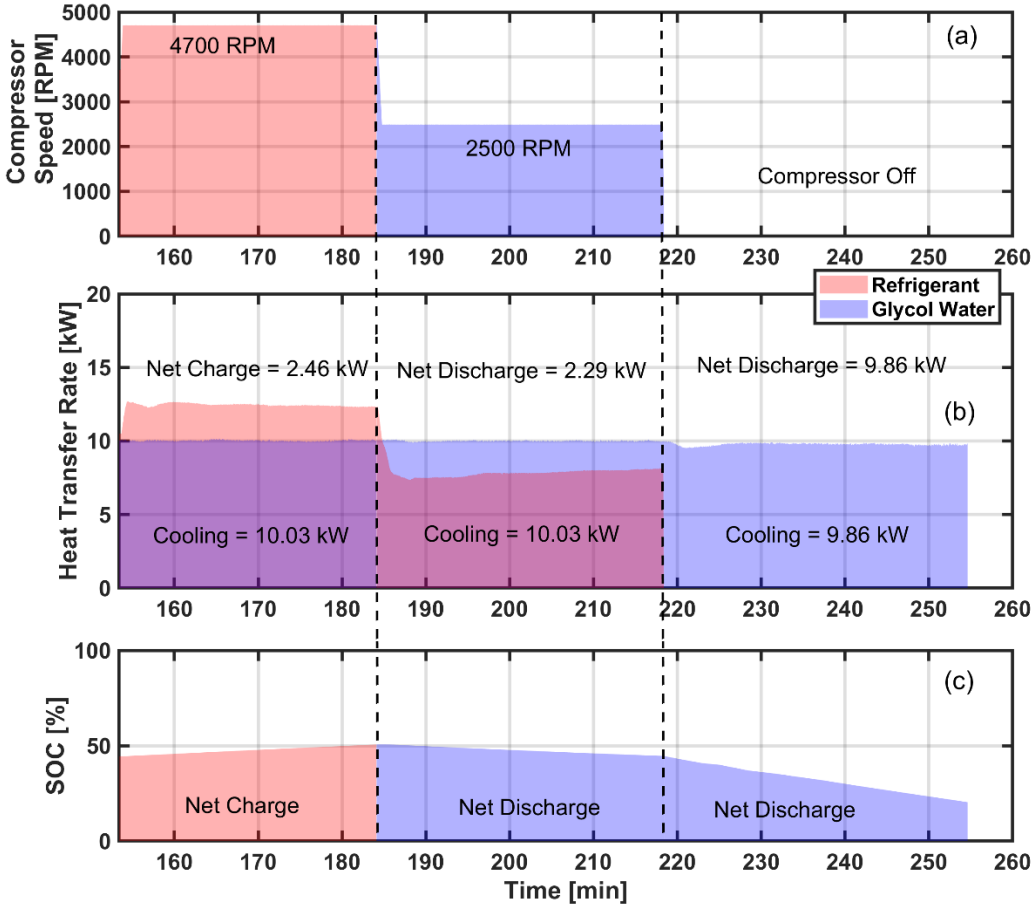

Figure 10: *Hybrid operation showing net charge (compressor at 4700 rpm), net discharge (2500 rpm), and full discharge (compressor off) (color shade pink shows charging using the refrigerant, and blue shows discharge using the glycol-water circuit)*

5. CONCLUSIONS

In this paper, we presented the design, fabrication, and performance evaluation of a dual-circuit PCM heat exchanger integrated with an air-conditioner. The modeled performance of this system indicates the potential of this technology to provide demand flexibility, including three potential values: 1.) Reduction in peak power and total energy required

during the peak demand period, 2) potential cost savings to customers and load reduction for electric utilities, and 3) flexible operation to meet on-peak periods of different durations, or at a different time of day. We also studied other operating modes including variable cooling capacity by only varying the airflow rate in the air-handling unit, and varying the compressor power input for load shaving. Based on our experiments and simulations, the thermal contact between the PCM and the fluid tubes is the major heat transfer resistance. Future designs will explore flat microchannels to minimize the thermal resistance and ease the manufacturing process. In conjunction with an improved design, increasing the PCM transition temperature can also improve the energy efficiency of the hybrid TES RTU.

NOMENCLATURE

Cp	specific heat	(kJ kg^{-1} $°C^{-1}$)
COP	coefficient of performance	(-)
EXV	electronic expansion valve	
HX	heat exchanger	
$\dot{m}$	mass flow rate	(kg s^{-1})
PCM	phase-change material	
$\dot{Q}$	heat transfer	(kW)
T	temperature	(°C)
$\dot{W}$	electric work	(kW)
Subscript		
cond	condenser	
comp	compressor	
glycol-water	coolant on discharge side	
in	inlet	
out	outlet	
ref	refrigerant	
th	thermal	

ACKNOWLEDGEMENT

This work was authored by the National Renewable Energy Laboratory, operated by Alliance for Sustainable Energy, LLC, for the U.S. Department of Energy (DOE) under Contract No. DE-AC36-08GO28308. Funding provided by the U.S. Department of Energy Office of Energy Efficiency and Renewable Energy Building Technologies Office. The views expressed in the article do not necessarily represent the views of the DOE or the U.S. Government. The U.S. Government retains and the publisher, by accepting the article for publication, acknowledges that the U.S. Government retains a nonexclusive, paid-up, irrevocable, worldwide license to publish or reproduce the published form of this work or allow others to do so, for U.S. Government purposes.

The authors also appreciate the financial and technical support for this research by the U.S. Department of Energy Technology Commercialization Fund and the program manager Antonio Bouza. We also appreciate the help of our collaborators, Dr. Said Al-Hallaj, Malek Nofal, David DiLoreto, and Mike Pintar at NETenergy, in fabricating the thermal energy storage module and providing insights into our experimental and analysis methods.

REFERENCES

[1] Maintaining Reliability in the Modern Power System. U.S. Department of Energy, 2016.

[2] CALMAC, http://www.calmac.com/.

[3] Mehling H, Cabeza LF. Heat and cold storage with PCM: Springer, 2008.

[4] Zhai XQ, Wang XL, Wang T, Wang RZ. A review on phase change cold storage in air-conditioning system: Materials and applications. Renewable and Sustainable Energy Reviews. 2013;22:108-20.

[5] Arteconi A, Hewitt NJ, Polonara F. State of the art of thermal storage for demand-side management. Applied Energy. 2012;93:371-89.

[6] Hasnain SM. Review on sustainable thermal energy storage technologies, Part II: cool thermal storage. Energy Conversion and Management. 1998;39:1139-53.

[7] Goyal A, Kozubal E, Woods J, Nofal M, Al-Hallaj S. Design and Performance Evaluation of a Dual-Circuit Thermal Energy Storage Module for Air Conditioners. Applied Energy (*In Press*).

[8] Mills A, Farid M, Selman JR, Al-Hallaj S. Thermal conductivity enhancement of phase change materials using a graphite matrix. Applied Thermal Engineering. 2006;26:1652-61.